J Biomol NMR (2012) 54:317–323
DOI 10.1007/s10858-012-9670-1

NMR STRUCTURE NOTE

NMR structure note: solution structure of human Miz-1 zinc fingers 8 to 10

Mikaël Bédard · Loïka Maltais · Marie-Eve Beaulieu · Josée Bilodeau · David Bernard · Pierre Lavigne

Received: 8 August 2012 / Accepted: 2 September 2012 / Published online: 18 September 2012

Biological context

The transcription factor Miz-1 (Myc-interacting zinc finger protein 1) is a member of the BTB/POZ protein family that contains around 40 human transcription factors. All these proteins bear an evolutionary conserved BTB protein–protein interaction domain at their N-terminus followed by a series of consecutive zinc finger motifs (ZF). Important roles in cell cycle regulation, development and cancer have been attributed to many BTB/POZ proteins demonstrating the relevance to understand the structural biology of those transcription factors (Kelly and Daniel 2006).

Miz-1 was first identified as a direct interactor of the oncogenic protein c-Myc by yeast two-hybrid (Peukert et al. 1997). Miz-1 plays a dual role on the expression of important cell cycle regulator genes such as the cyclin-dependent kinase inhibitors $p15^{INK4}$ (p15) and $p21^{CIP1}$ (p21) as it can either activate or repress them. Miz-1 acts as an activator of these cytostatic genes by recruiting the machinery necessary for their expression such as the histone acetyltransferase p300. On the other hand, it was reported that Miz-1 can also recruit c-Myc to the core promoter of its target genes causing their repression by abolishing the interaction of Miz-1 with its co-activator proteins (reviewed in Herkert and Eilers 2010).

While the structure of the BTB/POZ domain of Miz-1 has been resolved (Stead et al. 2007; Stogios et al. 2010), no structure for the 13 putative ZFs of Miz-1 has been reported yet. The specific DNA recognition of Miz-1 for its target gene promoters is believed to be mediated by its 13 ZFs. These small domains of approximately 30 amino acids are among the most abundant DNA-binding motifs in eukaryotes and possess a $\beta\beta\alpha$ fold that depend on the coordination of a Zn^{2+} atom by two Cys and two His side-chains. Based on known ZF-DNA complexes (reviewed in Pabo et al. 2001), it has been established that the recognition between ZFs and DNA is generally mediated by H-bonds between side-chains of residues −1, 2, 3 and 6 (position relative to the beginning of the α-helix) and bases in the Hoogsteen edge or the phosphate backbone of DNA. Normally, ZFs bind in the major groove of DNA in series of two or more, with each motif binding three to five bases, conferring a high binding specificity. Positional preferences have been deduced from known ZF-DNA complex structures and protein engineering. For instance, these studies have revealed that positively charged residues Arg at position −1 and 6 of the α-helix show a strong specificity for guanine whereas Asp at position −1 and 3 have a stringent preference for cytosine. These observed preferences led different groups to propose DNA recognition codes for C_2H_2 ZFs (Choo and Klug 1997; Desjarlais and Berg 1992; Wolfe et al. 2000). Whilst DNA sequences bound by Miz-1 have been identified at the proximal

M. Bédard · L. Maltais · M.-E. Beaulieu · J. Bilodeau · D. Bernard · P. Lavigne (✉)
Institut de Pharmacologie de Sherbrooke, Faculté de Médecine et des Sciences de la Santé, Université de Sherbrooke, 3001 12e Avenue Nord, Campus de la santé, Sherbrooke, QC J1H 5N4, Canada
e-mail: pierre.lavigne@usherbrooke.ca

M. Bédard · L. Maltais · M.-E. Beaulieu · J. Bilodeau · D. Bernard · P. Lavigne
Département de Biochimie, Faculté de Médecine et des Sciences de la Santé, Université de Sherbrooke, Sherbrooke, QC J1H 5N4, Canada

M. Bédard · L. Maltais · M.-E. Beaulieu · J. Bilodeau · D. Bernard · P. Lavigne
Regroupement Stratégique sur la Fonction, la Structure et l'Ingénierie des Protéines (PROTEO), Université Laval, Quebec, QC G1V 0A6, Canada

promoter of p15 and p21 (Lee et al. 2012; Seoane et al. 2002), the identity of the ZFs involved in these interactions is not known. In order to provide insights into this lack of knowledge about the structural biology of Miz-1, we have undertaken the determination of the solution structure of all 13 ZFs of Miz-1. Here, we report the NMR solution structure of ZFs 8 to 10.

Methods and results

Preparation of the Miz-1 ZF 8 to 10 construct (Miz8–10)

The cDNA fragment of ZFs 8 to 10 of Miz-1 (residues 500–581, Miz8–10) was generated by PCR from the complete cDNA of Miz-1 using primers F (5′-CATATGAAGCCCT ACGTGTGCATCCACTGCCAG-3′) and R (5′-GGATCC CTAGTCGTGGTGGCGAATATGATTGGCCAA-3′). The PCR product was inserted into pDrive (Qiagen) vector prior to a digestion by NdeI and BamHI. The digested product was inserted in pET-3a (Novagen) plasmid by the same restriction sites and the construct was transformed in BL21 star (DE3) competent cells (Invitrogen). Bacteria were grown in LB or in M9 broth containing $^{15}NH_4Cl$ and ^{13}C-glucose to an O.D. of 0.6 at 600 nm and were induced 15 h at 37 °C by the addition of IPTG (1 mM) and $ZnCl_2$ (0.1 mM) and harvested by centrifugation. The cell pellet was resuspended in a lysis buffer (700 mM NaCl, 50 mM KH_2PO_4, pH 4.5), frozen at −80 °C for at least 1 h prior to thawing in hot water and were then sonicated. The lysate was treated with 100 mM DTT and DNase I for an hour at 37 °C and was centrifuged at 17,500 RCF for 30 min. Soluble fraction was diluted 5 times in buffer A (0.5 M citric acid-Na_2HPO_4, pH 3, 8 M urea) and purified by FPLC with a HiTrap SP HP column (GE Healthcare). After an extensive wash with buffer B (0.5 M citric acid-Na_2HPO_4, pH 3), Miz8–10 was eluted by a gradient of NaCl. Ultracentrifugation (Amicon Ultra-15, Millipore) was used to concentrate the purified protein in H_2O containing 0.1 % trifluoroacetic acid (TFA). The protein was finally purified by HPLC with a Discovery BIO Wide Pore C18 column (Supelco) preconditioned with H_2O-0.1 % TFA and was eluted by a gradient of acetonitrile. The fractions containing purified Miz8–10 were lyophilized and kept a −20 °C until resuspension in the desired buffer.

NMR spectroscopy

Miz8–10 backbone and side-chain assignments were obtained by standard triple resonance experiments. NMR experiments were performed at 25 °C on a 600 MHz spectrometer (Varian INOVA). Samples were prepared at a final concentration of 0.75–1.00 mM in NMR buffer (10 mM acetic acid, 10 mM cacodylate, pH 6.5, 50 mM KCl, 2 mM TCEP, 3.5 eq. $ZnCl_2$, 10 % D_2O). 2D [^{15}N-^{1}H]-HSQC, and 3D HNCO, HNCACB, and CBCA (CO)NH spectra were used for the ^{1}H, ^{15}N, and ^{13}C assignments of the protein backbone. Side-chain ^{1}H and ^{13}C assignments were obtained using 2D [^{13}C-^{1}H]-HSQC, and 3D H(CCCO)NH, (H)CC(CO)NH and HCCH-TOCSY spectra. The ^{1}H and ^{13}C resonance assignments of the aromatic rings of Phe, Tyr and His were performed using 3D aliphatic and aromatic ^{13}C-edited NOESY-HSQC and ^{15}N-edited NOESY-HSQC. 3D NOESY spectra were recorded with mixing times of 50 and 150 ms. {^{1}H}-^{15}N heteronuclear values were calculated as the ratio between the cross-peak intensities with and without a ^{1}H saturation of 6 s. The NMR data were processed with the program NMRPipe and analyzed with the program CcpNmr Analysis.

Circular dichroism

Circular dichroism measurements were performed with a Jasco J-810 spectropolarimeter equipped with a Jasco Peltier-type thermostat. The CD spectra were recorded at 25 °C with 50 or 100 μM of Miz8–10 in CD buffer (10 mM acetic acid, 10 mM cacodylate, 50 mM KCl, 2 mM TCEP) at different pH and Zn^{2+} concentrations in a 1 mm quartz cell. CD spectra were obtained by averaging nine scans from 190 to 250 nm with a wavelength step of 0.2 nm and were smoothed using the program Spectra Manager. Data were converted from CD signal to mean residue ellipticity using the following equation: $[\theta] = (\delta \times MRW)/(10 \times c \times l)$ where δ is the ellipticity in degrees, MRW is the mean residue weight, c is the concentration of the sample (g ml^{-1}) and l is the path length (cm).

Folding of Miz8–10

Circular dichroism was used to optimize and characterize the folding of the Miz8–10 construct (Fig. 1a, b). Folding of C_2H_2 ZFs is normally both pH and zinc dependant since conserved His and Cys side-chains need to be in their deprotonated form to coordinate the Zn^{2+} atom (Fig. 1c). As expected, when raising the pH from 4 to 7 in excess of Zn^{2+}, the spectrum of the Miz8–10 construct switched from a random coil-like spectrum with a negative minimum around 200 nm to a more helical spectrum presenting two negative minima at 208 and 222 nm (Fig. 1a). The optimal folding of Miz8–10 was reached around pH 5 suggesting an important diminution of conserved Cys and His side-chains pKa, as already reported in other studies (Bombarda et al. 2002; Reddi et al. 2007). At pH 5.5, the addition of Zn^{2+} led to a transition from a CD spectrum

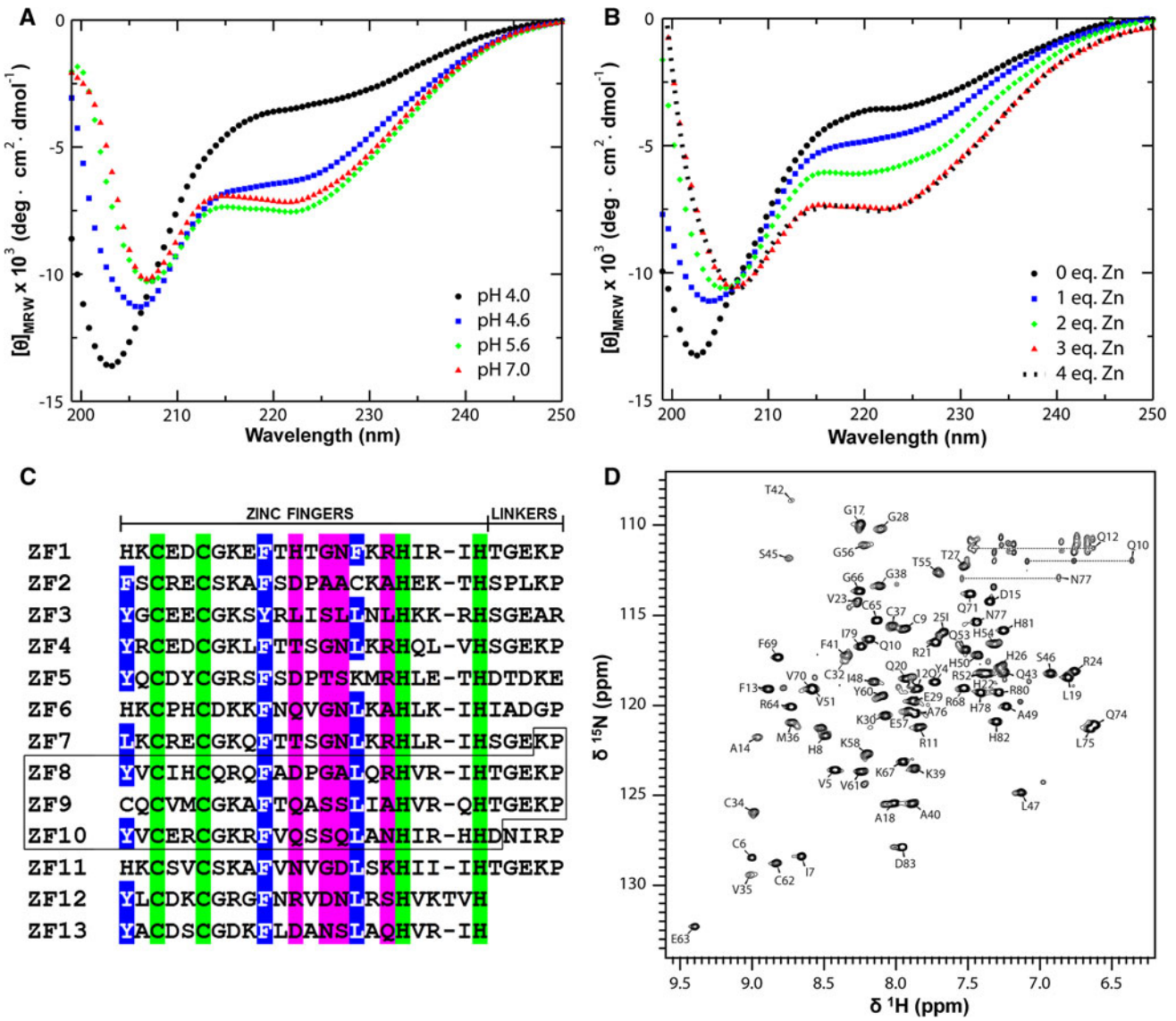

Fig. 1 Folding of Miz8–10. Miz8–10 Far-UV CD spectra recorded in excess of Zn^{2+} at different pH (**a**) or at pH 5.5 with different Zn^{2+} concentrations (**b**) demonstrating that the protein folding is both pH and Zn^{2+} dependent. **c** Amino acid sequence alignment of the 13 ZFs of Miz-1. Conserved residues involved in Zn^{2+} coordination are *colored* in *green*, conserved hydrophobic residues are in *blue* and residues potentially involved in DNA binding are in *magenta*. Residues contained in the Miz8–10 construct are *boxed*. **d** 2D [^{15}N-^{1}H]-HSQC spectrum of Miz8–10 showing the good peak dispersion obtained in the selected conditions used for NMR data collection. Amide resonances are labeled with the *one letter code*

typical of a random coil to an α-helix-like spectrum with a plateau at three molar equivalent of Zn^{2+}; suggesting that under these conditions, the three ZFs of Miz8–10 were well folded (Fig. 1b).

Resonance assignment, secondary structure analysis and dynamics of Miz8–10

To perform the resonance assignment of Miz8–10, a complete set of 2D and 3D NMR spectra were recorded. As expected from the CD study, the [^{15}N-^{1}H]-HSQC spectrum of the protein gave a well-dispersed peak pattern showing that the protein is well folded under the selected conditions (Fig. 1d). The good quality of spectra obtained for Miz8–10 allowed for the assignment of 96.1 % of $^{1}H_N$, 91.4 % of ^{15}N, 91.4 % of $^{13}C'$, 98.8 % of $^{13}C_\alpha$ and 98.7 % of $^{13}C_\beta$ for backbone atoms of residues 3–83. In addition, more than 80 % of all side-chain protons were assigned. All the NMR resonance assignments for Miz8–10 have been deposited in the BioMagResBank (BMRB ID: 18586).

The program DANGLE was used to obtain φ and ψ dihedral angles on the basis of backbone and $^{13}C_\beta$ chemical shift values. The 152 φ and ψ angles collected confirmed the anticipated $\beta\beta\alpha$ fold (except for the first β-strand in

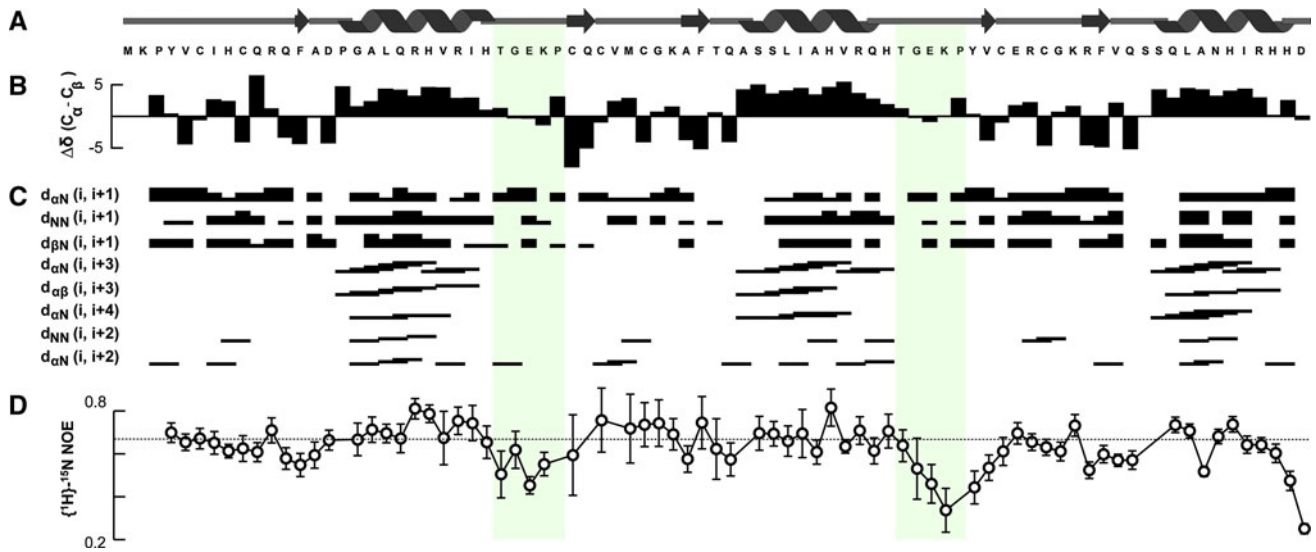

Fig. 2 Sequence specific secondary structure and $\{^1H\}$-^{15}N heteronuclear NOE values for Miz8–10. **a** Secondary structure predictions for Miz8–10 construct obtained from DANGLE. Secondary chemical shift values for C_α and C_β $\Delta\delta$ ($C_\alpha - C_\beta$) (**b**) along with NOE connectivities (**c**) and $\{^1H\}$-^{15}N heteronuclear NOE values (**d**) are shown and support the presence of the predicted secondary structures. Average calculated over $\{^1H\}$-^{15}N heteronuclear NOE values for ZF conserved residues (4–27, 32–54 and 60–82) is represented by a *dashed line*

ZF8) for the three ZFs of Miz8–10 (Fig. 2a). Moreover, the $\Delta\delta$ $C_\alpha - C_\beta$) values are negative and positive where the DANGLE results suggest the presence of β-strands and α-helices respectively (Fig. 2b). In addition, extensive sequential NOEs typical for α-helices are observed in these regions (Fig. 2c).

Analysis of $\{^1H\}$-^{15}N heteronuclear NOE values shows that, as reported elsewhere for other tandems of ZF, the backbone amides of the residues in the two canonical TGEKP linkers are more flexible than those in the ZF motifs (Fig. 2d) (Chou et al. 2010; Laity et al. 2000; Potter et al. 2005). Indeed, their NOE values are on average smaller (0.51 ± 0.09) than those in the ZFs (0.64 ± 0.09) indicating that they undergo fluctuation of larger amplitude on the pico- to nanosecond timescale (p value < 0.005). Moreover, only a few medium and no long range NOEs were observed for these segments corroborating that, in absence of DNA, canonical TGEKP linkers are flexible (Chou et al. 2010; Laity et al. 2000; Potter et al. 2005).

Solution structures of Miz-1 ZFs 8 to 10

Due to the flexibility of the linkers and the absence of medium and long range NOEs between ZFs of Miz8–10, the structure of each ZF was calculated separately. The NOE restraints, dihedral angles and hydrogen bonds used for structure calculations of each ZF are summarized in Table 1. All NOEs were assigned manually and converted into distance restraints using the program CcpNmr Analysis. Structure calculations were performed using the program ARIA in conjunction with CNS. The first run of calculations was performed without Zn^{2+}. The conformers with the lowest energy had the conserved Cys (residues 6, 9, 34, 37, 62 and 65) and His (residues 22, 26, 50, 54, 78 and 82) side-chains properly positioned at the motif interfaces to coordinate Zn^{2+} ions. In the subsequent runs of calculations a Zn^{2+} atom was added and distance restraints were imposed to respect a canonical coordination (2.3 Å for Zn^{2+}-S_γ and 2.0 Å for Zn^{2+}-$N_{\varepsilon 2}$). The 20 lowest-energy conformers out of 300 for the final iteration were refined in water and submitted to PROCHECK_NMR to validate the structural quality. The final structure ensembles of ZF8, ZF9 and ZF10 were deposited in the PDB under identification codes 2LVR, 2LVT and 2LVU, respectively.

The final ensembles for each ZF of Miz8–10 are shown in Fig. 3 (top). As can be seen, excellent definition was obtained from our set of restraints. Indeed, root mean square deviations (RMSD) of 0.23 ± 0.05 Å, 0.35 ± 0.06 Å and 0.31 ± 0.07 Å were calculated for backbone atoms of the conserved primary structure of ZF8 (residues 4–26), ZF9 (32–54) and ZF10 (60–82), respectively. The three motifs display the typical C_2H_2 ZF fold with a short β-hairpin followed by an α-helix. An excellent definition can be noticed for the side-chains coordinating the Zn^{2+} atoms (Figs. 1c, 3, green residues) and the side-chains of the conserved hydrophobic residues (Figs. 1c, 3, blue residues) at the interface of the β-hairpin and the α-helix except for Cys32 in ZF9. Indeed, compared to the more hydrophobic and bulkier side-chains of Tyr4 and Tyr60 present at the equivalent position, the Cys32 side-chain

Table 1 Structural statistics for ZFs 8 to 10 of Miz-1

	ZF 8	ZF 9	ZF 10
Restraints for final structure calculations			
NOE distance restraints			
Intraresidue ($\|i - j\| = 0$)	319	246	346
Sequential ($\|i - j\| = 1$)	159	122	145
Medium range ($1 < \|i - j\| < 5$)	77	54	81
Long range ($\|i - j\| \geq 5$)	56	36	70
Total NOE distance restraints	611	458	642
Hydrogen bonds	11 × 2	11 × 2	10 × 2
Zinc ligands	4 × 2	4 × 2	4 × 2
Dihedral angle restraints[a]			
Φ and ψ angles	52	54	46
χ angles	6	7	9
Structure statistics (20 structures)			
Number of NOE violations >0.5 Å	0	0	0
Number of dihedral angle violations >5°	0	0	0
RMS deviations from experimental data			
Average distance restraint violation (Å)	0.015 ± 0.001	0.027 ± 0.003	0.045 ± 0.002
Average dihedral restraint violation (°)	0.19 ± 0.14	0.37 ± 0.14	0.18 ± 0.11
RMS deviation to mean coordinates			
Backbone heavy atoms (Å)	1.15 ± 0.27	1.39 ± 0.39	0.60 ± 0.17
All heavy atoms (Å)	1.78 ± 0.26	2.00 ± 0.42	1.30 ± 0.17
For ZF consensus sequences[b]			
Backbone heavy atoms (Å)	0.23 ± 0.05	0.35 ± 0.06	0.31 ± 0.07
All heavy atoms (Å)	0.88 ± 0.10	0.86 ± 0.12	1.00 ± 0.10
Ramachandran plot statistics[c] (%)			
Residues in most favored regions			
Residues in additionally allowed regions	89.3	96.3	91.2
Residues in generously allowed regions	10.7	3.7	8.8
Residues in additionally allowed regions	0	0	0
Residues in disallowed regions	0	0	0

[a] Φ and ψ angles were derived from the program DANGLE

[b] ZF consensus sequences comprise residues 4–27 for ZF 8, 32–54 for ZF 9 and 60–82 for ZF 10

[c] Ramachandran plot statistics were generated using PROCHECK_NMR

does not converge to a well-defined conformation. Accordingly, it can be observed on Fig. 1d that its backbone amide cross-peak is broadened compared to those of Tyr4 and Tyr60 supporting the fact that Cys32 possibly experiences conformational exchange on the µs-ms time scale.

Discussion and conclusion

As expected, the side-chains at positions −1, 2, 3 and 6 of the α-helix involved in DNA binding by C_2H_2 ZFs of Miz-1 (Figs. 1c, 3, magenta residues) are solvent exposed and display more conformational flexibility in the free form of Miz8–10. Assuming a canonical binding and using the 1:1 DNA recognition code of C_2H_2 ZFs proposed by Wolf and collaborators (Wolfe et al. 2000), the DNA triplets predicted to be bound by the 13 Miz-1 ZFs are (starting from ZF 13): 5′-A(T/C)C NAG (G/T)CN NNA N(T/C)A GTC GAT NAA G(T/C)C GAT NNT NTC GA(T/C)-3′. Interestingly, the predicted target sequence of Miz8–10 (5′-NNA N(T/C)A GTC-3′) cannot be found in any of the sequences of p15 and p21 core promoters reported to be bound by Miz-1 (Lee et al. 2012; Seoane et al. 2002). This could indicate that ZFs 10–8 do not bind these promoters as a triplex. In fact, according to the predictions, ZFs 12–10 is the only triplex that could bind one of the reported site in p21 (actual sequence (AS): −76 5′-GAG GCG GGA-3′

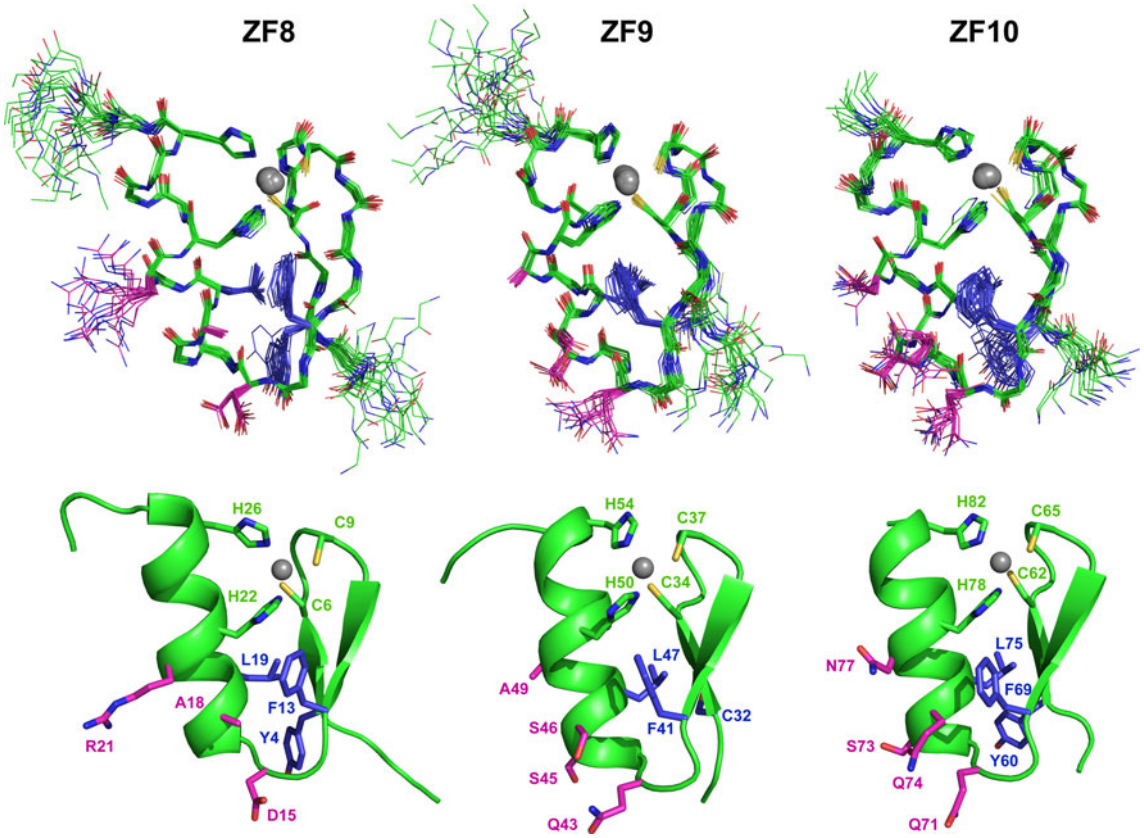

Fig. 3 NMR solution structure of Miz8–10. The best-fit superposition of the 20 final structures on the geometric average structure backbone atoms is shown at top for each ZF of Miz8–10. A *cartoon* representation of the structure presenting the lowest total energy for each ZF is shown at the bottom. Residues involved in the Zn^{2+} coordination are shown in *green*, conserved hydrophobic residues are in *blue* and residues potentially involved in DNA binding are shown in *magenta*. Zn^{2+} is represented by a *dark grey ball*

−84 vs. sequence predicted (SP): 5′-NAG (G/T)CN NNA-3′). Tandem 10–9 could also bind to the p21 core promoter (AS: −46 5′-ATA TCA-3′ −41 vs. SP : 5′-NNA N(T/C)A-3′). Again, according to the actual recognition code, only two tandems are susceptible to bind to the p15 promoter: ZFs 4–3 (AS: −150 5′-GAT GCT-3′ −155 vs. RC: 5′-GAT NNT-3′) and ZFs 10–9 (AS: −157 5′-CTA GCA-3′ −152 vs. RC: 5′-NNA N(T/C)A-3′). It is noteworthy, that both sequences are in the same region of the core promoter. Topologically, it seems highly improbable that both tandems would bind this sequences simultaneously. It also seems unlikely, that recognition of the p15 core promoter would rely on only one tandem of ZFs.

Failures and restrictions of the predictive power of the 1:1 recognition code have been discussed and documented elsewhere (Pabo et al. 2001; Segal and Barbas 2001). Indeed, issues such as binding site overlap, cooperativity and framework effects have to be considered when trying to rationalize specific ZF/DNA interactions. While the rational design and generation of polydactyl ZF proteins that bind to 5′-$(GNN)_n$-3′ with high affinity and specificity has been successful, specific targeting of the other DNA triplets is more challenging (Segal and Barbas 2001). Indeed, whilst the generation, by a combination phage display and site-directed mutagenesis, of a 6 ZF protein (Aart) that targets 5′-$(ANN)_6$-3′ has been rather successful (Dreier et al. 2001), it was later found to bind with more affinity to a more 5′G rich site (Segal et al. 2006). Moreover, the X-ray structure of the Aart/DNA complex further indicated that unlike 5′G selection by Arg side-chains, the 5′A, T and C is not specified by direct interactions with the side-chains at position 6 of the recognition helix (Segal et al. 2006). This result is rather counterintuitive and stresses the importance of solving more structures of ZF/DNA complexes with targets containing 5′A, T and C nucleotides and residues other than Arg at position 6 in the recognition helix in order to rationalize such a result. However, for the moment, neither the identification of *bona fide* consensus Miz-1 binding elements from its primary structure nor the identification of which ZF subset(s) binds to the p15 and p21 core promoters is possible. To address this, thermodynamical and structural approaches to characterize the affinity and specificity of Miz-1 ZFs subsets to known binding sites will be required. Such experiments are underway in our laboratory and these results will hopefully contribute to expand our

understanding of the rules of the DNA recognition by C_2H_2 ZFs and identify Miz-1 ZFs that bind to the p15 and p21 core promoters.

Acknowledgments This work was supported by the Natural Science and Engineering Research Council (NSERC) of Canada (grant to P.L. and studentships to M.B. and D.B.) and by the Regroupement stratégique sur la fonction, la structure et l'ingénierie des protéines (PROTEO). D.B. also acknowledges PROTEO for the award of graduate studentship. The authors thank Dr. Frank Hänel (Hans-Knöll-Institut für Naturstoff-Forschung e.V, Germany) for kindly providing us with the Miz-1 cDNA, Dr. Yves L. Dory (Université de Sherbrooke, Canada) for giving access and advice to use his HPLC system, Dr. Jean-François Naud for the initial cloning and Dr. Martin Montagne for his helpful comments on the manuscript. Finally, we wish to thank Prof. Jim Omichinski (U. de Montréal) for his help with the refolding protocol of Zinc Fingers.

References

Bombarda E, Cherradi H, Morellet N, Roques BP, Mely Y (2002) Zn(2+) binding properties of single-point mutants of the C-terminal zinc finger of the HIV-1 nucleocapsid protein: evidence of a critical role of cysteine 49 in Zn(2+) dissociation. Biochemistry 41:4312–4320

Choo Y, Klug A (1997) Physical basis of a protein-DNA recognition code. Curr Opin Struct Biol 7:117–125

Chou CC, Lou YC, Tang TK, Chen C (2010) Structure and DNA binding characteristics of the three-Cys(2)His(2) domain of mouse testis zinc finger protein. Proteins 78:2202–2212

Desjarlais JR, Berg JM (1992) Toward rules relating zinc finger protein sequences and DNA binding site preferences. Proc Natl Acad Sci USA 89:7345–7349

Dreier B, Beerli RR, Segal DJ, Flippin JD, Barbas CF III (2001) Development of zinc finger domains for recognition of the 5′-ANN-3′ family of DNA sequences and their use in the construction of artificial transcription factors. J Biol Chem 276:29466–29478

Herkert B, Eilers M (2010) Transcriptional repression: the dark side of myc. Genes Cancer 1:580–586

Kelly KF, Daniel JM (2006) POZ for effect—POZ-ZF transcription factors in cancer and development. Trends Cell Biol 16:578–587

Laity JH, Dyson HJ, Wright PE (2000) DNA-induced alpha-helix capping in conserved linker sequences is a determinant of binding affinity in Cys(2)-His(2) zinc fingers. J Mol Biol 295:719–727

Lee KM, Choi WI, Koh DI, Kim YJ, Jeon BN, Yoon JH, Lee CE, Kim SH, Oh J, Hur MW (2012) The proto-oncoprotein KR-POK represses transcriptional activation of CDKN1A by MIZ-1 through competitive binding. Oncogene 31:1442–1458

Pabo CO, Peisach E, Grant RA (2001) Design and selection of novel Cys2His2 zinc finger proteins. Annu Rev Biochem 70:313–340

Peukert K, Staller P, Schneider A, Carmichael G, Hanel F, Eilers M (1997) An alternative pathway for gene regulation by Myc. EMBO J 16:5672–5686

Potter BM, Feng LS, Parasuram P, Matskevich VA, Wilson JA, Andrews GK, Laity JH (2005) The six zinc fingers of metal-responsive element binding transcription factor-1 form stable and quasi-ordered structures with relatively small differences in zinc affinities. J Biol Chem 280:28529–28540

Reddi AR, Guzman TR, Breece RM, Tierney DL, Gibney BR (2007) Deducing the energetic cost of protein folding in zinc finger proteins using designed metallopeptides. J Am Chem Soc 129:12815–12827

Segal DJ, Barbas CF III (2001) Custom DNA-binding proteins come of age: polydactyl zinc-finger proteins. Curr Opin Biotechnol 12:632–637

Segal DJ, Crotty JW, Bhakta MS, Barbas CF III, Horton NC (2006) Structure of Aart, a designed six-finger zinc finger peptide, bound to DNA. J Mol Biol 363:405–421

Seoane J, Le HV, Massague J (2002) Myc suppression of the p21(Cip1) Cdk inhibitor influences the outcome of the p53 response to DNA damage. Nature 419:729–734

Stead MA, Trinh CH, Garnett JA, Carr SB, Baron AJ, Edwards TA, Wright SC (2007) A beta-sheet interaction interface directs the tetramerisation of the Miz-1 POZ domain. J Mol Biol 373:820–826

Stogios PJ, Cuesta-Seijo JA, Chen L, Pomroy NC, Prive GG (2010) Insights into strand exchange in BTB domain dimers from the crystal structures of FAZF and Miz1. J Mol Biol 400:983–997

Wolfe SA, Nekludova L, Pabo CO (2000) DNA recognition by Cys2His2 zinc finger proteins. Annu Rev Biophys Biomol Struct 29:183–212